Clinical Infectious Diseases

MAJOR ARTICLE

Role of Epithelial–Endothelial Cell Interaction in the Pathogenesis of Severe Acute Respiratory Syndrome Coronavirus 2 (SARS-CoV-2) Infection

Kenrie Pui-Yan Hui,[1,2] Man-Chun Cheung,[1] Ka-Ling Lai,[1] Ka-Chun Ng,[1] John Chi-Wang Ho,[1] Malik Peiris,[1,2] John Malcolm Nicholls,[3] and Michael Chi-Wai Chan[1,2]

[1]School of Public Health, Li Ka Shing Faculty of Medicine, University of Hong Kong, Hong Kong SAR, China; [2]Centre for Immunology and Infection, Hong Kong Science Park, Hong Kong SAR, China; and [3]Department of Pathology, Li Ka Shing Faculty of Medicine, University of Hong Kong, Hong Kong SAR, China

Background. The coronavirus disease 2019 (COVID-19) pandemic caused by the novel severe acute respiratory syndrome coronavirus 2 (SARS-CoV-2) continues to threaten public health globally. Patients with severe COVID-19 disease progress to acute respiratory distress syndrome, with respiratory and multiple organ failure. It is believed that dysregulated production of proinflammatory cytokines and endothelial dysfunction contribute to the pathogenesis of severe diseases. However, the mechanisms of SARS-CoV-2 pathogenesis and the role of endothelial cells are poorly understood.

Methods. Well-differentiated human airway epithelial cells were used to explore cytokine and chemokine production after SARS-CoV-2 infection. We measured the susceptibility to infection, immune response, and expression of adhesion molecules in human pulmonary microvascular endothelial cells (HPMVECs) exposed to conditioned medium from infected epithelial cells. The effect of imatinib on HPMVECs exposed to conditioned medium was evaluated.

Results. We demonstrated the production of interleukin-6, interferon gamma-induced protein-10, and monocyte chemoattractant protein-1 from the infected human airway cells after infection with SARS-CoV-2. Although HPMVECs did not support productive replication of SARS-CoV-2, treatment of HPMVECs with conditioned medium collected from infected airway cells induced an upregulation of proinflammatory cytokines, chemokines, and vascular adhesion molecules. Imatinib inhibited the upregulation of these cytokines, chemokines, and adhesion molecules in HPMVECs treated with conditioned medium.

Conclusions. We evaluated the role of endothelial cells in the development of clinical disease caused by SARS-CoV-2 and the importance of endothelial cell–epithelial cell interaction in the pathogenesis of human COVID-19 diseases.

Keywords. SARS-CoV-2; vascular endothelial cells; COVID-19; airway epithelial cells; pathogenesis.

A novel coronavirus, severe acute respiratory syndrome coronavirus 2 (SARS-CoV-2) emerged and caused human infection in 2019. Clinical manifestations of severe coronavirus disease 2019 (COVID-19) include sepsis, acute respiratory distress syndrome, and multiple organ failure [1, 2]. Autopsy analysis demonstrates correlations between inflammation and diffuse alveolar and endothelial dysfunction [2], indicating that there is an uncontrolled innate immune response that contributes to the severity of COVID-19. Published data show low induction of interferons (IFNs) by SARS-COV-2 infection in susceptible cells and in post-mortem lung tissues [3]. Since immune cells such as macrophages, which are potent cytokine inducers, do not support productive replication of SARS-CoV-2 virus in vitro, the source of proinflammatory cytokines and chemokines remains unclear. Endothelial cell damage has been reported in autopsy studies of COVID-19 [2]. Furthermore, plasma collected from patients with mild and severe COVID-19 led to damaged endothelial integrity [4]. Although a large number of treatment regimens have been tried, there is no approved specific therapeutic intervention for COVID-19 to date. A better understanding of the pathophysiology of COVID-19 in terms of the induction of proinflammatory immune responses thus provides important information to better identify targeted therapeutic strategies and reveal potential intervention targets.

Imatinib (also known as Gleevec) is a US Food and Drug Administration–approved drug for the treatment of patients with various types of leukemia and tumors [5] and is also an effective treatment for edema, inflammation, and vascular leakage in mouse models of acute lung injury [6, 7]. It also inhibits SARS-CoV and Middle East respiratory syndrome coronavirus (MERS)-CoV with low cytotoxicity [8]. Two phase 3 clinical trials to evaluate the use of imatinib to treat COVID-19 patients are in progress [9, 10], but there is not much information on the role of imatinib in SARS-CoV-2 infection, except for

Received 18 February 2021; editorial decision 27 April 2021; published online 6 May 2021.

Correspondence: Michael CW Chan, School of Public Health, LKS Faculty of Medicine, University of Hong Kong, L6-39, Laboratory Block, 21 Sassoon Road, Pokfulam, Hong Kong SAR, China (mchan@hku.hk).

Clinical Infectious Diseases® 2022;74(2):199–209

DOI: 10.1093/cid/ciab406

a single study that identified imatinib as an entry inhibitor of SARS-CoV-2 in lung and colonic organoids [11].

Well-differentiated human airway epithelial cells (wd-Calu-3) possess epithelial integrity and polarity with the development of a tight junction, cilia, and mucus secretion at the apical surface [12]. They are susceptible for both influenza viruses and SARS-CoV infection [13, 14]. In this study, we used wd-Calu-3 cells in an air–liquid interface (ALI) system to assess the viral replication, cytokine and chemokine production by the 3 pathogenic coronaviruses. We further demonstrate the interaction between pulmonary epithelial cells and endothelial cells during SARS-CoV-2 infection. Induction of cytokine and adhesion molecules from human pulmonary microvascular endothelial cells (HPMVECs) were detected via paracrine signaling by the treatment of conditioned medium from SARS-CoV-2–infected wd-Calu-3. Treatment with imatinib significantly reduced some of the elevated cytokines, chemokines, and adhesion molecules in these HPMVECs.

METHODS

Viruses

SARS-CoV-2 (BetaCoV/Hong Kong/VM20001061/2020, SCoV2) [15], SARS-CoV (strain HK39849/2003, SCoV) [15], MERS-CoV (human Erasmus Medical Center [EMC] prototype MERS-CoV, MCoV) [15], H5N1 virus isolated from a fatal human case (A/Hong Kong/483/1997, H5N1) [15], and pandemic influenza virus (A/Hong Kong/415742/2009, H1N1pdm) [15] were used (see Supplementary Materials). The experiments were carried out in a biosafety level 3 facility.

Differentiation of Calu-3 and Monolayer Calu-3 Culture

Human airway epithelial Calu-3 cells (American Type Culture Collection HTB-55), derived from human lung adenocarcinoma, were maintained in Dulbecco's modified Eagle's medium supplemented with 15% fetal bovine serum and 1% penicillin/streptomycin. Differentiation of Calu-3 cells was modified as reported previously [12, 16]. Cells were seeded on transwell inserts with 0.4-μm pore size at a density of 100 000. After reaching confluency, the cells were maintained at the ALI and the medium was changed every 48 hours. The wd-Calu-3 cultures were subjected to virus infection after 21 days of ALI culture.

Isolation and Maintenance of Endothelial Cells

HPMVECs were isolated from human lung tissues using anti-CD31-tagged dynabeads (Thermo Fisher) as described previously (see Supplementary Materials) [17, 18]. Cells were seeded on transwell inserts and subjected to infection or treatment after 5 days. The donor characteristics are listed in Supplementary Table 1. Approval to use human lung tissues was granted by the University of Hong Kong and the Hospital Authority (Hong Kong West) Institutional Review Board.

Virus Infection, Conditioned Medium Treatment, and Drug Treatment

Cells in transwell inserts were infected with viruses at a multiplicity of infection (MOI) of 0.1 for viral replication kinetics at the apical side or basolateral side. Viral titers in supernatant were determined using median tissue culture infectious dose ($TCID_{50}$) assay. Infection was done at MOI 2 and cell lysates were collected at 24 and 96 hours post-infection (hpi) for the mRNA expression using real-time polymerase chain reaction (RT-PCR) analysis. Mock-infected cells served as negative controls. At 96 hpi, cleaved-caspase 3 was stained.

Culture supernatants from the basolateral side of wd-Calu-3 cells infected with SARS-CoV-2 at a MOI of 2 for 96 hours were filtered. Mock-infected culture supernatants served as the control medium. HPMVECs were treated with conditioned medium from mock (CM-MK), SARS-CoV-2–infected cells (CM-SARS2), or directly infected by SARS-CoV-2 virus. HPMVECs were treated with cytomix—a mixture composed of interleukin (IL)-1β, tumor necrosis factor (TNF)-α, and IFN-γ at 50 ng/mL, which impaired epithelial integrity previously [19].

Detailed methods of virus infection, conditioned medium treatment and drug treatment, cytometric bead array (CBA), immunofluorescence staining of caspase-3, quantitative RT-PCR, and statistical analysis are described in Supplementary Materials.

RESULTS

SARS-CoV-2 Predominantly Releases Infectious Virus Particles from the Apical Surface of Human Airway Epithelial Cells

We developed wd-Calu-3 and directly compared the viral replication efficiency of 3 human coronaviruses, SARS-CoV-2, SARS-CoV, and MERS-CoV, together with 2 influenza A control viruses, pandemic H1N1 and highly pathogenic avian H5N1 viruses, which replicate efficiently in wd-Calu-3. The latter shows a high cytokine induction phenotype [20]. Viral titers of SARS-CoV-2 increased by 4 $\log_{10}$ at the apical side at 24 hours post-infection, which was significantly higher than for SARS-CoV and MERS-CoV but similar to that of H1N1 and H5N1 (Figure 1A). By calculating the area under curve (AUC) from 24- to 72-hour viral titers, SARS-CoV-2 had a viral replication efficiency similar to that of SARS-CoV (Figure 1B). Both SARS-CoV-2 and SARS-CoV had a lower viral replication efficiency than the 2 influenza viruses (Figure 1B). A relatively low level of infectious viral titers was detected in the basolateral side (Figure 1C, 1D). Monolayers of Calu-3 did not support replication of SARS-CoV-2 or SARS-CoV, but MERS-CoV, H1N1, and H5N1 viruses replicated to titers more than 10^6 $TCID_{50}$/mL and had higher AUCs than SARS-CoV-2 and SARS-CoV (Supplementary Figure 1A, 1B). When compared with monolayers of Calu-3 cells, the expression of angiotensin-converting enzyme 2 (ACE2), human airway trypsin-like protease (HAT), and transmembrane protease serine 2 (TMPRSS2) was 20-, 2.9-, and 2.3-fold in wd-Calu-3 cells (Supplementary Figure 2).

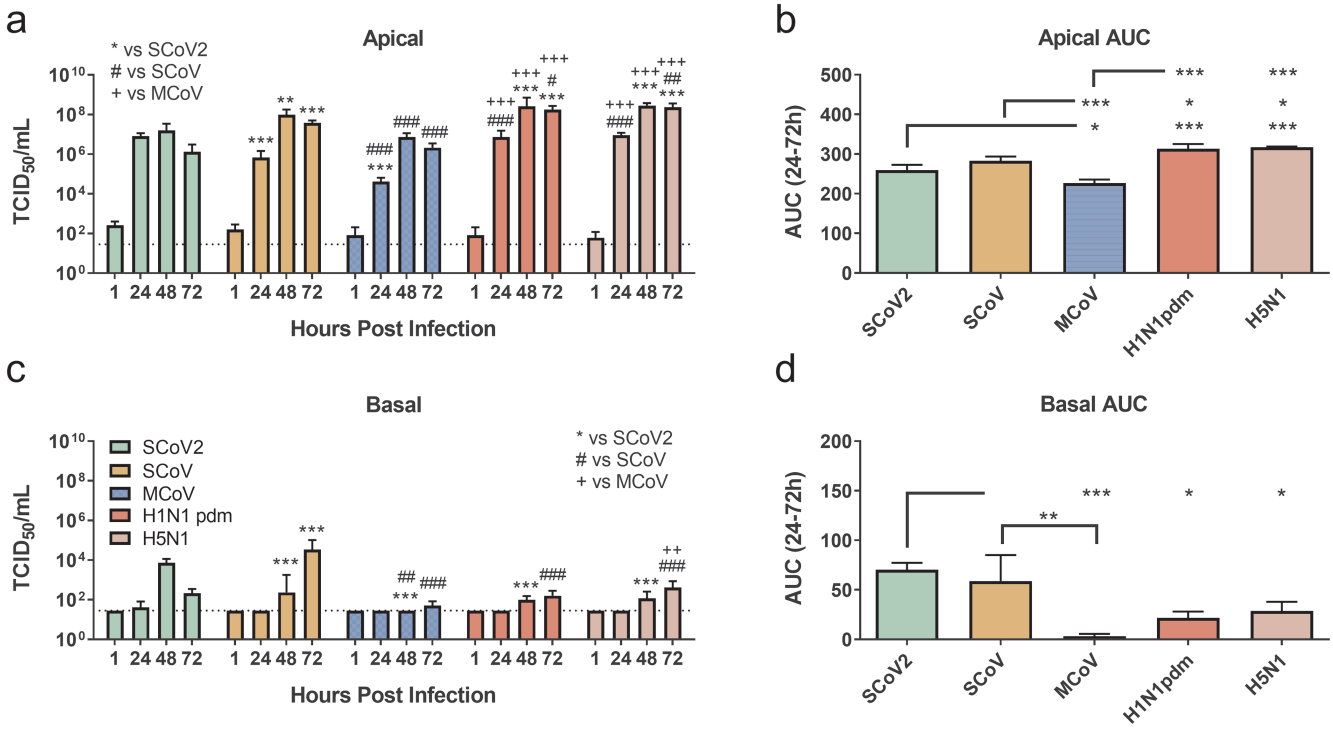

Figure 1. Viral replication kinetics of coronaviruses and influenza A viruses in well-differentiated-Calu-3 (wd-Calu-3) cells. wd-Calu-3 cells were infected with SCoV2, SCoV, MCoV, H1N1pdm, and H5N1 viruses at multiplicity of infection 0.1 from the apical side. Viral load in culture supernatants from the apical compartment (*A* and *B*) and basal compartment (*C* and *D*) were determined at indicated time points by $TCID_{50}$. *A* and *C*, Graphs show the mean virus titer pooled from 3 independent experiments ± standard deviation of the mean. The horizontal dotted line denotes the limit of detection in the $TCID_{50}$ assay. *, $P < .05$; **, $P < .01$; ***, $P < .001$, compared with SCoV2; #, $P < .05$; ##, $P < .01$; ###, $P < .001$, compared with SCoV; +, $P < .05$; ++, $P < .01$; +++, $P < .001$, compared with MCoV. *B* and *D*, Graphs show the AUC (24–72 hours) with data points pooled from 3 independent experiments ± standard deviation of the mean. *, $P < .05$; **, $P < .01$; ***, $P < .001$. Abbreviations: AUC, area under the curve; H1N1pdm, pandemic influenza A; H5N1, influenza A H5N1; MCoV, Middle East respiratory syndrome coronavirus; SCoV, severe acute respiratory syndrome coronavirus; SCoV2, severe acute respiratory syndrome coronavirus 2; TCID, tissue culture infectious dose.

Cytokine and Chemokine Production by SARS-CoV-2 at the Basolateral Side of the Airway Epithelium

Kumaki et al reported that SARS-CoV produces chemokine interferon gamma-induced protein (IP)-10 in Calu-3 cells and that the expression peaks at 96 hours after infection [21]. Therefore, we measured proinflammatory cytokine and chemokine production after infection at MOI 2. At 96 hours post-infection, but not at 24 hours (data not shown), SARS-CoV-2 released higher levels of IL-6, IP-10, and monocyte chemoattractant protein-1 (MCP-1) in the basal compartment than in the apical chamber, while H1N1 did the reverse. H5N1 had similar levels of IP-10 and regulated on activation normal T-cells expressed and secreted (RANTES) in both surfaces, while IL-6 and TNF had higher concentrations in the apical chamber than in the basal chamber (Supplementary Figure 3).

SARS-CoV-2 released higher levels of IL-6 and IP-10 from the basal compartment than the other 2 coronaviruses and H1N1 and had a higher MCP-1 concentrations than MERS-CoV and H1N1 (Figure 2). However, SARS-CoV-2 induced less IL-6, IP-10, RANTES, and TNF when compared with H5N1 (Figure 2). It also induced less MCP-1 from the apical side than H1N1 and less IL-6, IP-10, RANTES, and TNF than H5N1 (Figure 2). In monolayer Calu-3 cells, H5N1 induced the highest levels of IL-6, IP-10, and RANTES among all the tested viruses (Supplementary Figure 1C). The expression of cleaved-caspase 3, which is an apoptotic cell death marker, was assessed by immunofluorescence staining in both mock and SARS-CoV-2–infected wd-Calu-3 cells at MOI 0.1 or 2 for 96 hours. Percentages of cells with caspase 3 staining were similar between mock and SARS-CoV-2–infected cells (Supplementary Figure 4).

IFN and IFN-Stimulated Gene Profile in SARS-CoV-2–Infected Airway Epithelium

Both SARS-CoV-2 and SARS-CoV upregulated the mRNA expression of IFN-β, IFN-λ1, interferon-stimulated gene 15 (ISG15), and myxovirus resistance protein 1 (MxA) at 24 hours post-infection in wd-Calu-3 cells (Figure 3A–3E). However, SARS-CoV-2 induced higher expression of these genes and the viral gene (*ORF1b*) than SARS-CoV and MERS-CoV. Higher expression of *IFN-β* was found in SARS-CoV than MERS-CoV–infected cells, while MERS-CoV induced higher level of ISG15 than SARS-CoV (Figure 3B, 3D). The expression of viral

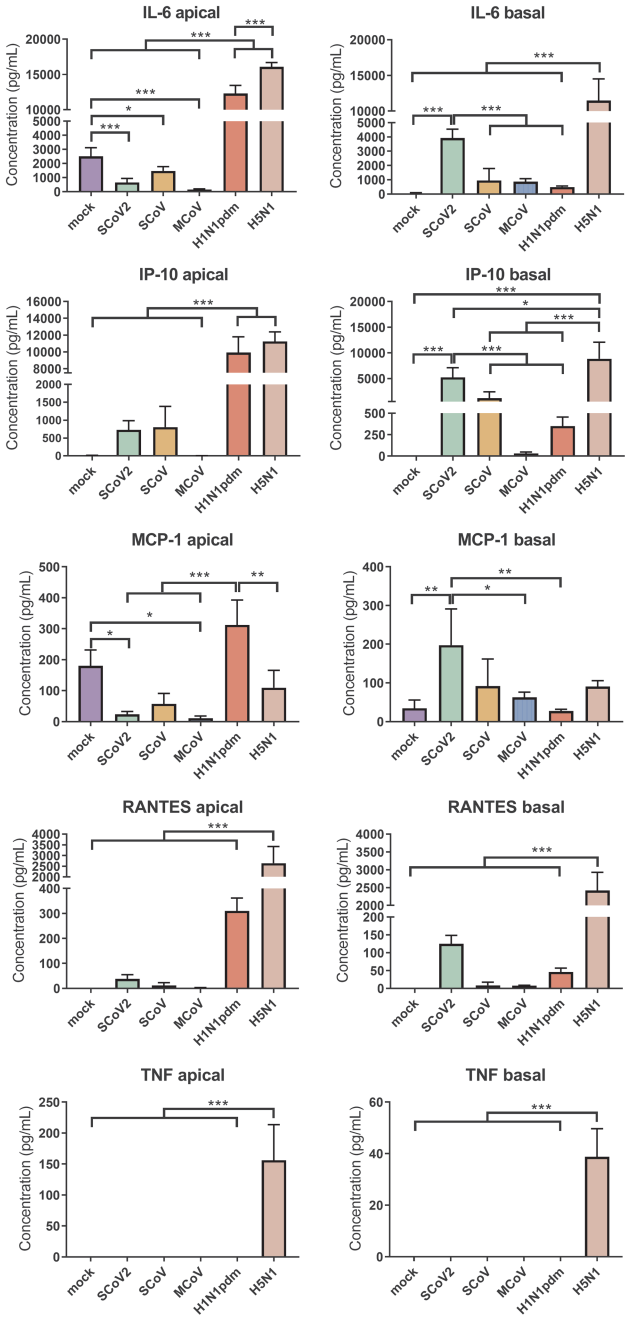

Figure 2. Production of cytokines and chemokines by SCoV2 in well-differentiated Calu-3 (wd-Calu-3) cells. wd-Calu-3 cells were infected with SCoV2, SCoV, MCoV, H1N1pdm, and H5N1 viruses at multiplicity of infection 2 from the apical side. At 96 hours post-infection, concentrations of cytokines and chemokines in the culture supernatants from both apical and basal chambers were measured by cytometric bead assay. Results are the calculated mean from 3 independent experiments ± standard deviation of the mean. *, $P < .05$; **, $P < .01$; ***, $P < .001$. Abbreviations: H1N1pdm, pandemic influenza A; H5N1, influenza A H5N1; IL, interleukin; IP, interferon gamma induced protein; MCoV, Middle East respiratory syndrome coronavirus; MCP, monocyte chemoattractant protein; RANTES, regulated on activation normal T-cells expressed and secreted; SCoV, severe acute respiratory syndrome coronavirus; SCoV2, severe acute respiratory syndrome coronavirus 2; TNF, tumor necrosis factor.

genes was similar between SARS-CoV and SARS-CoV-2 at 96 hours post-infection (Figure 3F). SARS-CoV-2 and MERS-CoV upregulated the mRNA expression of *IFN-β*, *IFN-λ1*, *ISG15*, *MxA*, *IL28-receptor α (RA)2*, and *RA3*, while only SARS-CoV-2 upregulated the expression of *IL28-RA1* (Figure 3G–3M). SARS-CoV induced lower expression levels of *IFN-β* and *ISG15* than SARS-CoV-2, while there was no significant differences in *MxA* level among the 3 viruses (Figure 3G, 3I, 3J).

The mRNA expression of *ACE2*, the receptor of SARS-CoVs, was dramatically suppressed by SARS-CoV-2 infection as early as 24 hours and at 96 hours post-infection (Supplementary Figure 5A, 5D). A similar level of suppression of *ACE2* expression was observed in SARS-CoV-2– and SARS-CoV–infected cells at 96 hours post-infection (Supplementary Figure 5A, 5D). *HAT* expression was upregulated by MERS-CoV infection only (Supplementary Figure 5B, 5E), while the expression of *TMPRSS2* was not affected (Supplementary Figure 5C, 5F).

Nonproductive Replication of SARS-CoV-2 in HPMVECs

Direct infection of HPMVECs with SARS-CoV-2 or SARS-CoV led to less than 1 $\log_{10}$ increase in titers irrespective of apical or basolateral side infection (Figure 4A, 4C). In contrast, the 2 control viruses, MERS-CoV and H5N1, had significantly higher viral titers as early as 24 hours post-infection (Figure 4A, 4C) from either apical or basolateral infection. Peak viral titers of MERS-CoV increased more than 3 $\log_{10}$ from both the apical and basolateral side, while H5N1 virus was mainly released from the apical side (Figure 4A, 4C). MERS-CoV and H5N1 had significantly higher viral replication efficiencies in terms of AUC than SARS-CoV-2 and SARS-CoV in HPMVECs, except for the insignificant H5N1 virus release from the basolateral side when infection was performed at the basolateral surface (Figure 4B, 4D).

Paracrine Induction of Proinflammatory Cytokines and Leukocyte Adhesion Molecules in HPMVECs

We collected the conditioned medium from SARS-CoV-2 or mock-infected wd-Calu-3 cells from the basal chamber at 96 hours post-infection and treated HPMVECs. Direct infection of HPMVECs with SARS-CoV-2 was included for parallel comparison. We found that SARS-CoV-2–conditioned medium induced significantly higher mRNA expression levels of proinflammatory cytokines (*IL-6* and *IP-10*) and biomarkers associated with vascular leakage, including *vascular cell adhesion molecule-1* (*VCAM-1*) and *endothelial leukocyte adhesion molecule* (*E-selectin*), at 3 hours post-treatment when compared with mock-conditioned medium-treated cells (Figure 5A–5D). Virus infection induced mRNA expression of *E-selectin* and *vascular endothelial growth factor-A* (*VEGF-A*), although there was no evidence of productive replication in these cells (Figure 5D, 5E).

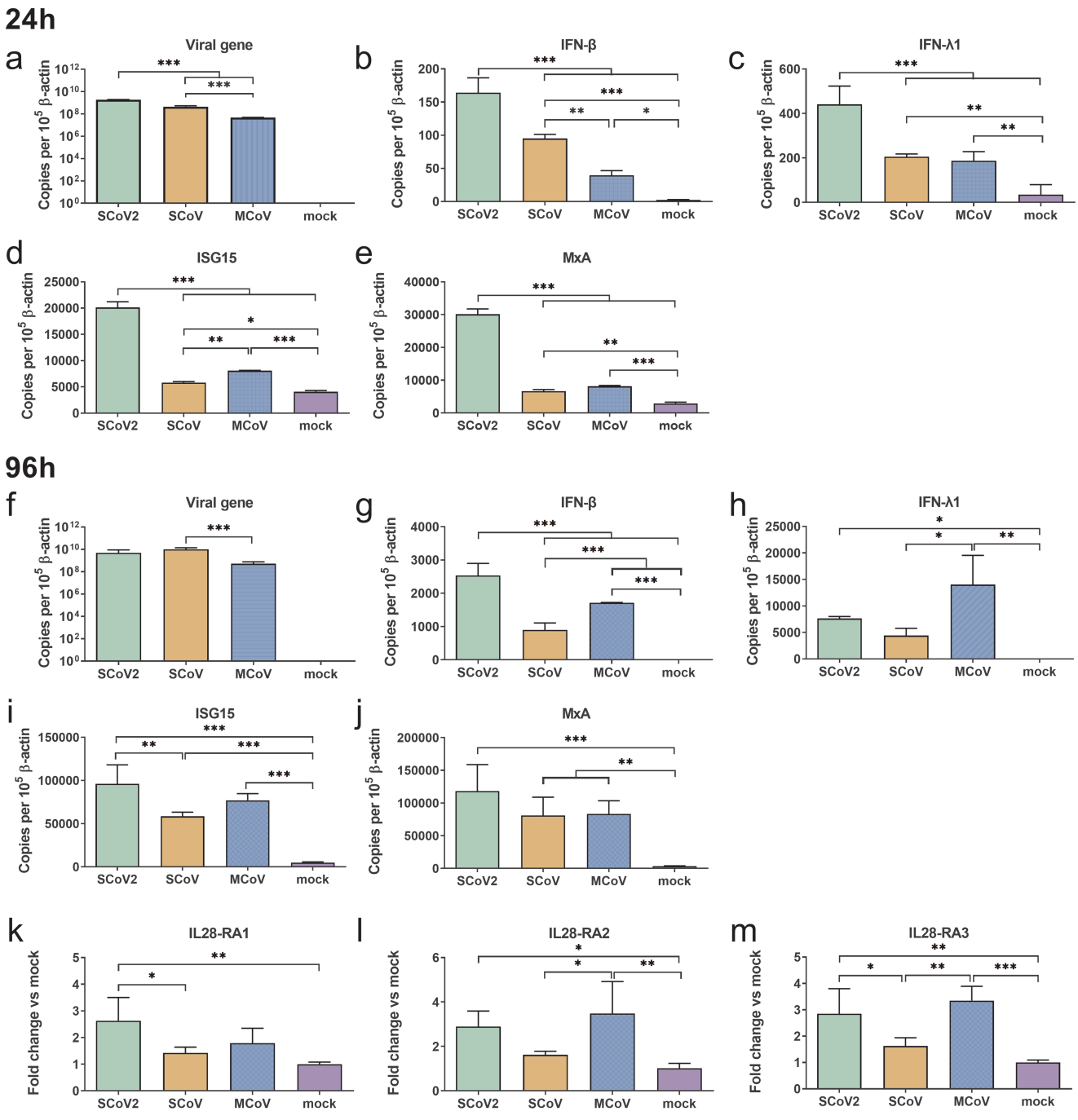

Figure 3. Induction of IFNs, ISGs, and IL-28 receptors by coronaviruses and influenza A viruses in well-differentiated Calu-3 (wd-Calu-3) cells. wd-Calu-3 cells were infected with SCoV2, SCoV, and MCoV viruses at multiplicity of infection 2 from the apical side. The mRNA expression of the viral gene (ORF1b gene of SCoV2 and SCoV; UpE gene of MCoV), IFN-β, IFN-λ1, ISG15, and MxA after 24 hours (*A* to *E*) and 96 hours (*F* to *J*) infection of SCoV2, SCoV, and MCoV were monitored using real-time PCR (polymerase chain reaction). *K* to *M*, The mRNA expressions of IL28-receptor alpha (RA)-1, RA-2, and RA-3 by virus infection for 96 hours were measured using real-time PCR. Results are the calculated mean from 3 independent experiments ± standard deviation of the mean. *, $P < .05$; **, $P < .01$; ***, $P < .001$. Abbreviations: IFN, interferon; IL, interleukin; ISG, interferon-stimulated gene; MCoV, Middle East respiratory syndrome coronavirus; MxA, myxovirus resistance protein 1; SCoV, severe acute respiratory syndrome coronavirus; SCoV2, severe acute respiratory syndrome coronavirus 2.

Treatment lasting 24 hours with SARS-CoV-2–conditioned medium upregulated the mRNA expression of proinflammatory cytokines and chemokines (*MCP-1*, *IL-1β*, *IL-6*, *IL-8*, and *IP-10*; Figure 5F–5J) and biomarkers associated with vascular leakage (*E-selectin, VCAM-1*, *angiopoietin (Ang)-1, and Ang-2*; Figure 5K–5N). Moreover, the upregulation of *VCAM-1* increased from 8-fold to 17-fold from 3 hours to 24 hours post-treatment (Figures 3L, 5C). Cytomix treatment on

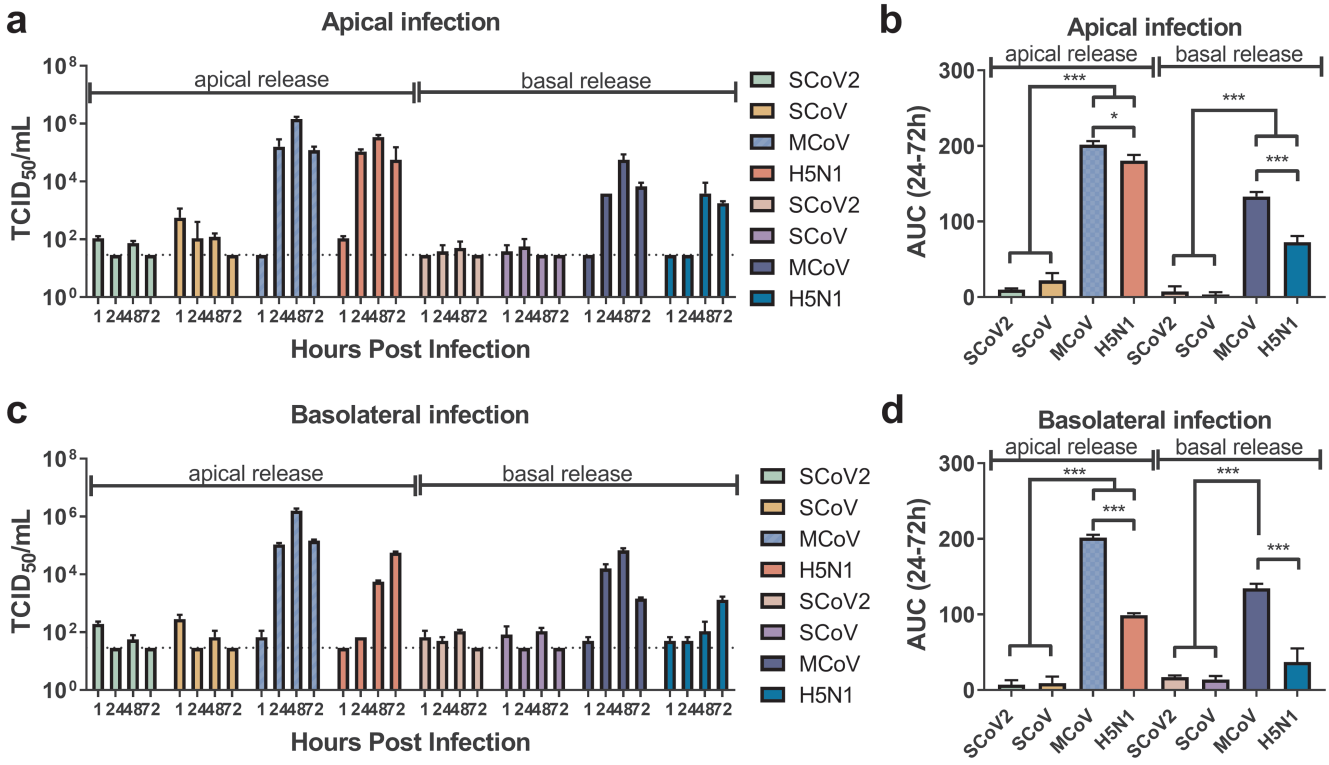

Figure 4. Viral replication kinetics of coronaviruses and influenza A viruses in human primary pulmonary microvascular endothelial cells (HPMVECs). HPMVECs were infected with SCoV2, SCoV, MCoV, and H5N1 viruses at multiplicity of infection 0.1 from the apical (*A* and *B*) or basolateral (*C* and *D*) side. Viral load in culture supernatants from apical and basolateral compartments were determined at indicated time points by $TCID_{50}$. *A* and *C*, Graphs show the mean virus titer pooled from 3 individual donors ± standard deviation of the mean. The horizontal dotted line denotes the limit of detection in $TCID_{50}$. *B* and *D*, Graphs show the area under curve (24–72 hours) with data points from 3 individual donors ± standard deviation of the mean. *, $P < .05$; **, $P < .01$; ***, $P < .001$. Abbreviations: H5N1, influenza A H5N1; MCoV, Middle East respiratory syndrome coronavirus; SCoV, severe acute respiratory syndrome coronavirus; SCoV2, severe acute respiratory syndrome coronavirus 2; $TCID_{50}$, tissue culture infectious dose.

HPMVECs upregulated tested cytokines, chemokines, and biomarkers with higher magnitudes compared with SARS-CoV-2–conditioned medium, except a downregulation of Ang-2 was observed (Supplementary Figure 6). Except for the directly infected cells, there was no viral ORF1b gene of SARS-CoV-2 detected in cells treated with conditioned media after 24 hours incubation (Supplementary Figure 7). HPMVECs treated with the conditioned medium did not enhance the infection of SARS-CoV-2, demonstrated by a similar level of the ORF1b gene (Supplementary Figure 8A) and no detection of infectious particles by $TCID_{50}$ assay (data not shown). IP-10 was upregulated in cells treated with SARS-CoV-2–conditioned medium and subsequently infected with SARS-CoV-2 (Supplementary Figure 8B).

The induction of *IL-6, MCP-1, IP-10, VCAM-1*, and *E-selectin*, but not *IL-8*, by SARS-CoV-2–conditioned medium treatment was significantly suppressed by treatment with imatinib (Figure 6) at a noncytotoxic concentration in HPMVECs (Supplementary Figure 9).

DISCUSSION

Clinical manifestations of SARS-CoV-2–infected patients have been attributed to abnormal cytokine release, the so-called cytokine storm, especially those with severe disease [22]. The production of proinflammatory cytokines and chemokines has been demonstrated in airway epithelial cells after SARS-CoV-2 infection [23]. Even though damage to the endothelium in severe COVID-19 has been demonstrated [24–27], the interaction between respiratory epithelial and endothelial cells during SARS-CoV-2 infection is not fully understood, and there is a lack of information on the active role of endothelial cells in contributing to the disease progression.

Wd-Calu-3 cells supported more robust productive replication of SARS-CoV-2 and SARS-CoV than undifferentiated Calu-3 cells, and viruses were mainly released from the apical side. The higher expression of ACE2 in wd-Calu-3 than undifferentiated Calu-3 cells may explain the differential susceptibilities of the 2 models to SARS-CoV-2 infection. More importantly, we found robust cytokine and chemokine production

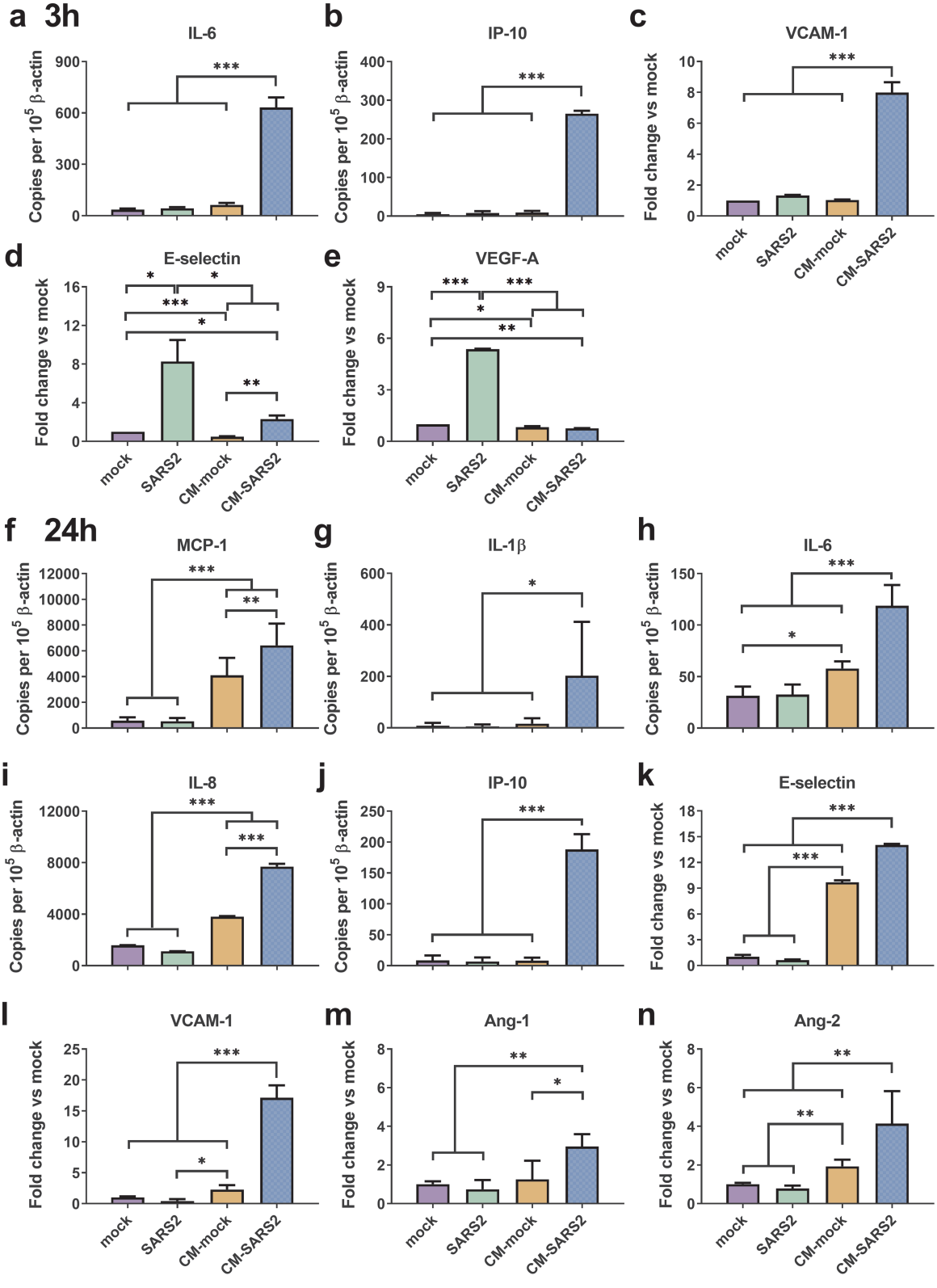

Figure 5. Paracrine effects of severe acute respiratory syndrome coronavirus 2 (SARS-CoV-2)–conditioned medium from Calu-3 cells on human primary pulmonary microvascular endothelial cells (HPMVECs). HPMVECs were treated with CM-MK and CM-SARS2 collected at 96 hours post-infection of SARS2 infection. Cell lysates were harvested at 3 hours (*A* to *E*) and 24 hours (*F* to *N*) post-treatment with conditioned medium or direct infection for determination of mRNA expression of IL-6, IP-10, MCP-1, IL-1β, IL-8, VCAM-1, E-selectin, VEGF-A, Ang-1, and Ang-2. Results are the calculated mean from 3 individual donors ± standard deviation of the mean. *, $P < .05$; **, $P < .01$; ***, $P < .001$. Abbreviations: Ang, angiopoietin; CM-MK, conditioned medium from mock; CM-SARS2, conditioned medium from severe acute respiratory syndrome coronavirus 2–infected cells; E-selectin, endothelial leukocyte adhesion molecule; IL, interleukin; IP, interferon gamma induced protein; MCP, monocyte chemoattractant protein; VCAM, vascular cell adhesion molecule; VEGF-A, vascular endothelial growth factor-A.

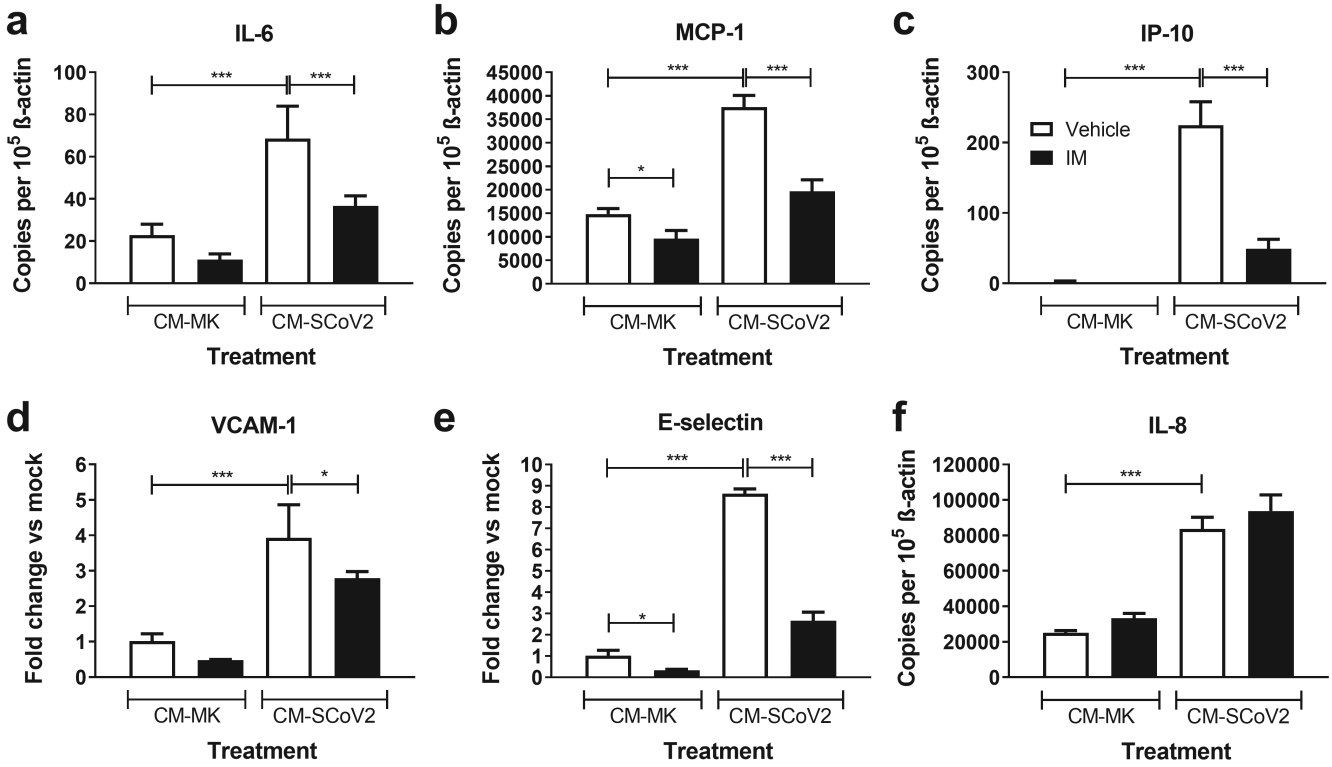

Figure 6. Inhibitory effects of imatinib on cytokines, chemokines, and adhesion molecules induction in human primary pulmonary microvascular endothelial cells (HPMVECs) treated with severe acute respiratory syndrome coronavirus 2–conditioned medium. HPMVECs were treated with CM-MK or CM-SCoV2 collected at 96 hours post-infection in the presence or absence of imatinib (IM) for 24 hours. Cell lysates were harvested for the mRNA expression measurement of IL-6, MCP-1, IP-10, VCAM-1, E-selectin, and IL-8. Results are the calculated mean from 3 individual donors ± standard deviation of mean. *, $P < .05$; **, $P < .01$; ***, $P < .001$. Abbreviations: CM-MK, conditioned medium from mock; CM-SCoV2, conditioned medium from severe acute respiratory syndrome coronavirus 2–infected cells; E-selectin, endothelial leukocyte adhesion molecule; IL, interleukin; IP, interferon gamma induced protein; MCP, monocyte chemoattractant protein; VCAM, vascular cell adhesion molecule.

at the basolateral side, including IL-6, IP-10, and MCP-1, by SARS-CoV-2 infection at 96 hours post-infection. Although production of IL-6 and IP-10 by SARS-CoV-2 was lower than that following infection by H5N1, a number of reports indicate that these cytokines and chemokines are associated with disease severity of COVID-19 [28–30]. Therefore, airway epithelial cells are most likely one of the sources of proinflammatory cytokines and chemokines with clinically important roles in the pathogenesis of COVID-19 in SARS-CoV-2 infection. These findings are in line with reports using primary human airway epithelial cultures [23, 31].

There is a lack of information on direct comparison of the innate immune responses induced by the 3 coronaviruses. Undetectable IFN mRNA was reported in monolayer cultures of human primary airway epithelial cells (HBEC) after SARS-CoV-2 infection [3, 23]. In *ex vivo* human lung explants, SARS-CoV-2 failed to induce IFNs up to 48 hours post-infection, while SARS-CoV induced detectable IFN mRNA at 48 hours [32]. However, in line with our findings, induction of IFN-β and IFN-λ mRNA was observed in SARS-CoV-2–infected differentiated HBEC [33] and Calu-3 cells [34, 35]. These discrepancies could be explained by the cell type-specific phenotypes, differences in infectious dosage, and time points after infection since we used the ALI model of Calu-3 cells and we aimed at infecting the cells in a synchronizing manner with a high MOI. Our findings reveal that SARS-CoV-2 induced a more robust innate immune response than SARS-CoV and MERS-CoV as early as 24 hours; the differential expression was also seen at 96 hpi in wd-Calu-3 cells.

There were minimal cytopathic effects in SARS-CoV-2–infected cells up to 96 hours post-infection. This phenotype provides long periods of time for virus release and cytokine and chemokine production. Dramatic downregulation of ACE2 was observed in SARS-CoV-2–infected cells. This is in line with Patra's report that the protein expression of ACE2 is downregulated upon SARS-CoV-2 infection in human lung epithelial and liver epithelial cells [36]. The loss of ACE2 at the cell surface abolishes the degradation of extracellular angiotensin II, which is supported by the markedly increased level of angiotensin II in the plasma samples from COVID-19 patients [37]. A number of studies demonstrated that SARS-CoV infection downregulated ACE2 expression, resulting in increased

angiotensin II levels in blood samples; this contributed to acute lung injury [38, 39].

Dysfunction of endothelial cells has been frequently reported in severe COVID-19 [24–27]. Virus particles were occasionally found in endothelial cells of COVID-19 patients in an autopsy study [27]. However, we found that by using human primary pulmonary endothelial cells [40], there was no productive replication of SARS-CoV-2 in HPMVECs following infection from the apical or basolateral side of the endothelium nor in HPMVECs pretreated with conditioned medium from SARS-CoV-2–infected airway cells. These findings suggest that although SARS-CoV-2 virus can enter endothelial cells, it is not able to produce infectious viral particles. This is in line with reports that used an immortalized human endothelial cell line and umbilical vein endothelial cells [41].

There are several reports of the cross-talk between lung epithelial and endothelial cells upon exposure to SARS-CoV-2 virus or protein. A recent study reported the induction of IL-6 via spike protein expression in A549 cells and the induction of MCP-1 in liver endothelial cells by supernatants from the SARS-CoV-2 spike protein-transfected A549 cells [36]. Another study showed the disruption of intracellular organelles after SARS-CoV-2 infection in both human lung epithelial cells and immortalized pulmonary endothelial cells in a co-culture system, while the damage to endothelial cells is via an indirect manner [42]. Damaged barrier function after prolonged SARS-CoV-2 infection in umbilical vein endothelial cells was also reported in a human chip model composed of nondifferentiated Calu-3, endothelial, and mononuclear cells [41]. In contrast to the reports mentioned above, our study applied a more physiologically relevant cell model using of differentiated Calu-3 in an ALI system and primary HPMVECs. Furthermore, live virus was used to infect from the apical side of the airway epithelial cells. We believe our findings reflect a more physiological interaction between airway epithelial cells and pulmonary endothelial cells. In line with the studies of Deinhardt, induction of proinflammatory and type I and III IFN responses by SARS-CoV-2 was observed in airway epithelial cells [41]. However, we also compared cytokine and chemokine production by SARS-CoV-2 with other pathogenic respiratory viruses. Nonproductive replication of SARS-CoV-2 in endothelial cells was observed in both studies. More importantly, only our findings reveal the active contribution of endothelial cells to the pathogenesis of COVID-19 via the induction of leukocyte adhesion molecules and vascular leakage biomarkers. We demonstrated that treatment with a conditioned media from SARS-CoV-2–infected airway cells that contained proinflammatory cytokines and chemokines, but not the virus, in HPMVECs caused the elevation of proinflammatory cytokine, chemokine (including MCP-1, IL-1β, IL-6, IL-8, and IP-10), and a number of molecules involved in vascular leakage and dysfunction (including E-selectin, VCAM-1, and Ang-2) [43–48]. These findings suggest that the soluble mediators secreted from infected airway cells have a more important impact on endothelial cells in production of proinflammatory immune responses than SARS-CoV-2 virus infection. These findings are supported by the results from cytomix treatment composed of IL-1β, TNF-α, and IFN-γ, which upregulated the tested genes listed above, except Ang-2. Therefore, these findings reveal that endothelial cells play a role in orchestrating the cytokine induction and upregulation of adhesion molecules, which may recruit immune cells to the inflammation sites and further elevate the production of proinflammatory immune responses and, in turn, contribute to the pathogenesis of COVID-19.

The robust expression of E-selectin and VEGF-A in endothelial cells 3 hours following SARS-CoV-2 inoculation suggests that these changes may be induced via virus infection processes including virus attachment, cell entry, and fusion with the host cell membrane, while the induction of E-selectin, VCAM-1, Ang-1, and Ang-2 could be induced by soluble factors of SARS-CoV-2–conditioned medium. The signaling pathways that lead to the induction of these vascular leakage markers in the context of SARS-CoV-2 infection warrant further study.

Imatinib has been studied in 2 phase 3 clinical trials as a treatment for COVID-19 patients [9, 10]. However, there is limited information on the role of imatinib and SARS-CoV-2 infection. Apart from antiviral effects, we report that imatinib can act as an immunomodulator as it significantly reduced the induction of proinflammatory cytokines, chemokines, and leukocyte adhesion molecules in endothelial cells treated with conditioned medium from SARS-CoV-2–infected airway cells. The antiinflammatory effects observed are in line with a number of in vivo acute lung injury studies that used imatinib as a therapeutic strategy [49, 50]. In lipopolysaccharides (LPS) and ventilator-induced lung injury study, imatinib decreased bronchoalveolar lavage protein, immune cell influx, and TNF-α levels in mice [6]. Our findings highlight the antiinflammatory effect of imatinib in endothelial cells during SARS-CoV-2 infection.

In summary, we showed nonproductive replication of SARS-CoV-2 in HPMVECs. However, HPMVECs may play an active and important role in orchestrating the cytokine storm, recruiting leukocytes, and contributing to vascular damage through epithelial–endothelial cell interaction. Furthermore, we demonstrated the immunomodulatory role of imatinib during SARS-CoV-2 infection, which supports its use for the treatment of COVID-19. This study not only demonstrates the cross-talk of pulmonary epithelial–endothelial cells but also reveals the important role of endothelial cells in the pathogenesis of human SARS-CoV-2 infection.

Supplementary Data

Supplementary materials are available at *Clinical Infectious Diseases* online. Consisting of data provided by the authors to benefit the reader, the posted materials are not copyedited and are the sole responsibility of the authors, so questions or comments should be addressed to the corresponding author.

Notes

Acknowledgments. We acknowledge Rachel Ching in the School of Public Health and Kevin Fung in the Department of Pathology, University of Hong Kong, for their technical support. R Fouchier, Erasmus University Medical Center, Rotterdam, provided the Middle East respiratory syndrome coronavirus.

Disclaimer. The funding sources had no role in writing the manuscript or in the decision to submit it for publication. The authors have not been paid to write this article by a pharmaceutical company or other agency. The authors had full access to all the data in the study and had final responsibility for the decision to submit for publication.

Financial support. This work was supported by grants from the National Institute of Allergy and Infectious Diseases (contract HHSN272201400006C), Research Grant Council of Hong Kong (T11-712/19-N), and the Health and Medical Research Fund (COVID190202 and 15141022).

Potential conflicts of interest. All authors: No reported conflicts of interest. All authors have submitted the ICMJE Form for Disclosure of Potential Conflicts of Interest. Conflicts that the editors consider relevant to the content of the manuscript have been disclosed.

References

1. Zhou F, Yu T, Du R, et al. Clinical course and risk factors for mortality of adult inpatients with COVID-19 in Wuhan, China: a retrospective cohort study. Lancet **2020**; 395:1054–62.
2. D'Errico S, Zanon M, Montanaro M, et al. More than pneumonia: distinctive features of SARS-Cov-2 infection. From autopsy findings to clinical implications: a systematic review. Microorganisms **2020**; 8:1642–59.
3. Blanco-Melo D, Nilsson-Payant BE, Liu WC, et al. Imbalanced host response to SARS-CoV-2 drives development of COVID-19. Cell **2020**; 181:1036–45.e9.
4. Michalick L, Weidenfeld S, Grimmer B, et al. Plasma mediators in patients with severe COVID-19 cause lung endothelial barrier failure. Eur Respir J **2021**; 57:2002384.
5. US Food and Drug Administration. GLEEVEC® (imatinib mesylate) tablets label. Available at: https://www.accessdata.fda.gov/drugsatfda_docs/label/2016/021588s047lbl.pdf. Accessed 18 February 2021).
6. Rizzo AN, Sammani S, Esquinca AE, et al. Imatinib attenuates inflammation and vascular leak in a clinically relevant two-hit model of acute lung injury. Am J Physiol Lung Cell Mol Physiol **2015**; 309:L1294–304.
7. Aman J, van Bezu J, Damanafshan A, et al. Effective treatment of edema and endothelial barrier dysfunction with imatinib. Circulation **2012**; 126:2728–38.
8. Dyall J, Coleman CM, Hart BJ, et al. Repurposing of clinically developed drugs for treatment of Middle East respiratory syndrome coronavirus infection. Antimicrob Agents Chemother **2014**; 58:4885–93.
9. Emadi A, Chua JV, Talwani R, Bentzen SM, Baddley J. Safety and efficacy of imatinib for hospitalized adults with COVID-19: a structured summary of a study protocol for a randomised controlled trial. Trials **2020**; 21:897.
10. Duvignaud A, Lhomme E, Pistone T, et al.; COVERAGE Study Group. Home treatment of older people with symptomatic SARS-CoV-2 infection (COVID-19): a structured summary of a study protocol for a multi-arm multi-stage (MAMS) randomized trial to evaluate the efficacy and tolerability of several experimental treatments to reduce the risk of hospitalisation or death in outpatients aged 65 years or older (COVERAGE trial). Trials **2020**; 21:846.
11. Han Y, Duan X, Yang L, et al. Identification of SARS-CoV-2 inhibitors using lung and colonic organoids. Nature **2021**; 589:270–5.
12. Liu YC, Hussain F, Negm O, et al. Contribution of the alkylquinolone quorum-sensing system to the interaction of *Pseudomonas aeruginosa* with bronchial epithelial cells. Front Microbiol **2018**; 9:3018.
13. Yoshikawa T, Hill TE, Yoshikawa N, et al. Dynamic innate immune responses of human bronchial epithelial cells to severe acute respiratory syndrome-associated coronavirus infection. PLoS One **2010**; 5:e8729.
14. Grantham ML, Wu WH, Lalime EN, Lorenzo ME, Klein SL, Pekosz A. Palmitoylation of the influenza A virus M2 protein is not required for virus replication in vitro but contributes to virus virulence. J Virol **2009**; 83:8655–61.
15. Hui KPY, Cheung MC, Perera RAPM, et al. Tropism, replication competence, and innate immune responses of the coronavirus SARS-CoV-2 in human respiratory tract and conjunctiva: an analysis in ex-vivo and in-vitro cultures. Lancet Respir Med **2020**; 8:687–95.
16. Stewart CE, Torr EE, Mohd Jamili NH, Bosquillon C, Sayers I. Evaluation of differentiated human bronchial epithelial cell culture systems for asthma research. J Allergy (Cairo) **2012**; 2012:943982.
17. van Beijnum JR, Rousch M, Castermans K, van der Linden E, Griffioen AW. Isolation of endothelial cells from fresh tissues. Nat Protoc **2008**; 3:1085–91.
18. Alphonse RS, Vadivel A, Zhong S, et al. The isolation and culture of endothelial colony-forming cells from human and rat lungs. Nat Protoc **2015**; 10:1697–708.
19. Chan MC, Kuok DI, Leung CY, et al. Human mesenchymal stromal cells reduce influenza A H5N1-associated acute lung injury in vitro and in vivo. Proc Natl Acad Sci U S A **2016**; 113:3621–6.
20. Zeng H, Pappas C, Katz JM, Tumpey TM. The 2009 pandemic H1N1 and triple-reassortant swine H1N1 influenza viruses replicate efficiently but elicit an attenuated inflammatory response in polarized human bronchial epithelial cells. J Virol **2011**; 85:686–96.
21. Kumaki Y, Day CW, Bailey KW, et al. Induction of interferon-gamma-inducible protein 10 by SARS-CoV infection, interferon alfacon 1 and interferon inducer in human bronchial epithelial Calu-3 cells and BALB/c mice. Antivir Chem Chemother **2010**; 20:169–77.
22. Huang C, Wang Y, Li X, et al. Clinical features of patients infected with 2019 novel coronavirus in Wuhan, China. Lancet **2020**; 395:497–506.
23. Vanderheiden A, Ralfs P, Chirkova T, et al. Type I and type III interferons restrict SARS-CoV-2 infection of human airway epithelial cultures. J Virol **2020**; 94:e00985–20.
24. Pons S, Fodil S, Azoulay E, Zafrani L. The vascular endothelium: the cornerstone of organ dysfunction in severe SARS-CoV-2 infection. Crit Care **2020**; 24:353.
25. Morris G, Bortolasci CC, Puri BK, et al. The pathophysiology of SARS-CoV-2: a suggested model and therapeutic approach. Life Sci **2020**; 258:118166.
26. Zhang J, Tecson KM, McCullough PA. Endothelial dysfunction contributes to COVID-19-associated vascular inflammation and coagulopathy. Rev Cardiovasc Med **2020**; 21:315–9.
27. Ackermann M, Verleden SE, Kuehnel M, et al. Pulmonary vascular endothelialitis, thrombosis, and angiogenesis in Covid-19. N Engl J Med **2020**; 383:120–8.
28. Chen Y, Wang J, Liu C, et al. IP-10 and MCP-1 as biomarkers associated with disease severity of COVID-19. Mol Med **2020**; 26:97.
29. Hue S, Beldi-Ferchiou A, Bendib I, et al. Uncontrolled innate and impaired adaptive immune responses in patients with COVID-19 acute respiratory distress syndrome. Am J Respir Crit Care Med **2020**; 202:1509–19.
30. Ruan Q, Yang K, Wang W, Jiang L, Song J. Clinical predictors of mortality due to COVID-19 based on an analysis of data of 150 patients from Wuhan, China. Intensive Care Med **2020**; 46:846–8.
31. Elkahloun AG, Saavedra JM. Candesartan could ameliorate the COVID-19 cytokine storm. Biomed Pharmacother **2020**; 131:110653.
32. Chu H, Chan JF, Wang Y, et al. Comparative replication and immune activation profiles of SARS-CoV-2 and SARS-CoV in human lungs: an ex vivo study with implications for the pathogenesis of COVID-19. Clin Infect Dis **2020**; 71:1400–9.
33. Ravindra NG, Alfajaro MM, Gasque V, et al. Single-cell longitudinal analysis of SARS-CoV-2 infection in human airway epithelium identifies target cells, alterations in gene expression, and cell state changes. PLoS Biol **2021**; 19:e3001143.
34. Sun J, Ye F, Wu A, et al. Comparative transcriptome analysis reveals the intensive early stage responses of host cells to SARS-CoV-2 infection. Front Microbiol **2020**; 11:593857.
35. Lei X, Dong X, Ma R, et al. Activation and evasion of type I interferon responses by SARS-CoV-2. Nat Commun **2020**; 11:3810.
36. Patra T, Meyer K, Geerling L, et al. SARS-CoV-2 spike protein promotes IL-6 trans-signaling by activation of angiotensin II receptor signaling in epithelial cells. PLoS Pathog **2020**; 16:e1009128.
37. Liu Y, Yang Y, Zhang C, et al. Clinical and biochemical indexes from 2019-nCoV infected patients linked to viral loads and lung injury. Sci China Life Sci **2020**; 63:364–74.
38. Huang F, Guo J, Zou Z, et al. Angiotensin II plasma levels are linked to disease severity and predict fatal outcomes in H7N9-infected patients. Nat Commun **2014**; 5:3595.
39. Imai Y, Kuba K, Rao S, et al. Angiotensin-converting enzyme 2 protects from severe acute lung failure. Nature **2005**; 436:112–6.
40. Chan LLY, Hui KPY, Kuok DIT, et al. Risk assessment of the tropism and pathogenesis of the highly pathogenic avian influenza A/H7N9 virus using ex vivo and in vitro cultures of human respiratory tract. J Infect Dis **2019**; 220:578–88.
41. Deinhardt-Emmer S, Böttcher S, Häring C, et al. SARS-CoV-2 causes severe epithelial inflammation and barrier dysfunction. J Virol **2021**; 95:e00110–21.
42. Wang P, Luo R, Zhang M, et al. A cross-talk between epithelium and endothelium mediates human alveolar-capillary injury during SARS-CoV-2 infection. Cell Death Dis **2020**; 11:1042.
43. Paulus P, Jennewein C, Zacharowski K. Biomarkers of endothelial dysfunction: can they help us deciphering systemic inflammation and sepsis? Biomarkers **2011**; 16 Suppl 1:S11–21.
44. Karlsson S, Pettilä V, Tenhunen J, Lund V, Hovilehto S, Ruokonen E; Finnsepsis Study Group. Vascular endothelial growth factor in severe sepsis and septic shock. Anesth Analg **2008**; 106:1820–6.

45. van der Flier M, van Leeuwen HJ, van Kessel KP, Kimpen JL, Hoepelman AI, Geelen SP. Plasma vascular endothelial growth factor in severe sepsis. Shock **2005**; 23:35–8.
46. Dvorak HF, Brown LF, Detmar M, Dvorak AM. Vascular permeability factor/vascular endothelial growth factor, microvascular hyperpermeability, and angiogenesis. Am J Pathol **1995**; 146:1029–39.
47. Orfanos SE, Kotanidou A, Glynos C, et al. Angiopoietin-2 is increased in severe sepsis: correlation with inflammatory mediators. Crit Care Med **2007**; 35:199–206.
48. Ricciuto DR, dos Santos CC, Hawkes M, et al. Angiopoietin-1 and angiopoietin-2 as clinically informative prognostic biomarkers of morbidity and mortality in severe sepsis. Crit Care Med **2011**; 39:702–10.
49. Chilakapati SR, Serasanambati M, Vissavajjhala P, Kanala JR, Chilakapati DR. Amelioration of bleomycin-induced pulmonary fibrosis in a mouse model by a combination therapy of bosentan and imatinib. Exp Lung Res **2015**; 41:173–88.
50. Chan RW, Chan MC, Wong AC, et al. DAS181 inhibits H5N1 influenza virus infection of human lung tissues. Antimicrob Agents Chemother **2009**; 53:3935–41.